High-temperature Piezoelectric Conversion using Thermally Stabilized Electrospun Polyacrylonitrile Membranes†

Wenyu Wang[a,1], Yide Zheng[a,1], Yue Sun[a], Xin Jin*[b], Jiarong Niu[a], Maoyun Cheng[a], Hongxia Wang*[c], Hao Shao[c], Tong Lin*[c]

[a] State Key Laboratory of Separation Membranes and Membrane Processes, School of Textile Science and Engineering, Tiangong University, Tianjin 300387, P. R. China.
[b] State Key Laboratory of Separation Membranes and Membrane Processes, School of Materials Science and Engineering, Tiangong University, Tianjin 300387, P. R. China
[c] Institute for Frontier Materials, Deakin University, Geelong, Victoria 3216, Australia

[1] Both authors contributed equally to the manuscript.

Corresponding authors' emails: jinxin29@126.com; hong.wang@deakin.edu.au; tong.lin@deakin.edu.au,

Electronic Supplementary Information

Table S1 Mechanical-to-electrical conversion of polymers at high temperatures

Types	Active layers	Peak Voltage (V)	d_{33} (pC N^{-1})	Maximum operating temperature (℃)	Refs
piezoelectric	PVDF/$BaTiO_3$ composite	-	40	100	[1]
	Polyimide (PI)/(Bi,La)FeO_3-$PbTiO_3$ 0-3 composite	110	290	300	[2]
	Flexible polyimide/3D $PbTiO_3$ flower composites	140	-	300	[3]
	Crosslinked P(VDF-TrFE)/C_{60} composites	-	31	140	[4]
	aluminum nitride/polyimide composite	-	8.3	300	[5]
	PVDF/2,6(β-CN)APB/ODPA (poli 2,6) polyimide	0.0796	-	200	[6]
Triboelectric	PTFE film-aluminum foil	38	-	227	[7]
	Polyacrylonitrile nanofibers-graphene oxide nanosheets	80	-	200	[8]
	polybenzazole aerogels	32	-	350	[9]
Electret	Polyimide	1	-	120	[10]
	Carbon fiber/polymer-matrix structural composite	1.2	-	70	[11]
	Polycarbonate films	-	28	100	[12]
	Cyclo-olefin polymers and copolymers	-	15	110	[13]
	Heat-treated Polyacrylonitrile Membranes	9.7 （62*）	80	550	This work

***** Measured by an oscilloscope (Yokogawa DL350) with an internal resistance of 100 MΩ.

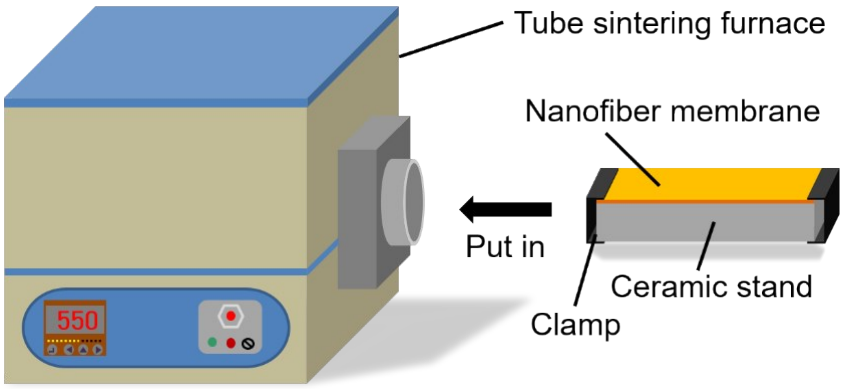

Fig. S1 devices for heat treatment of PAN membranes.

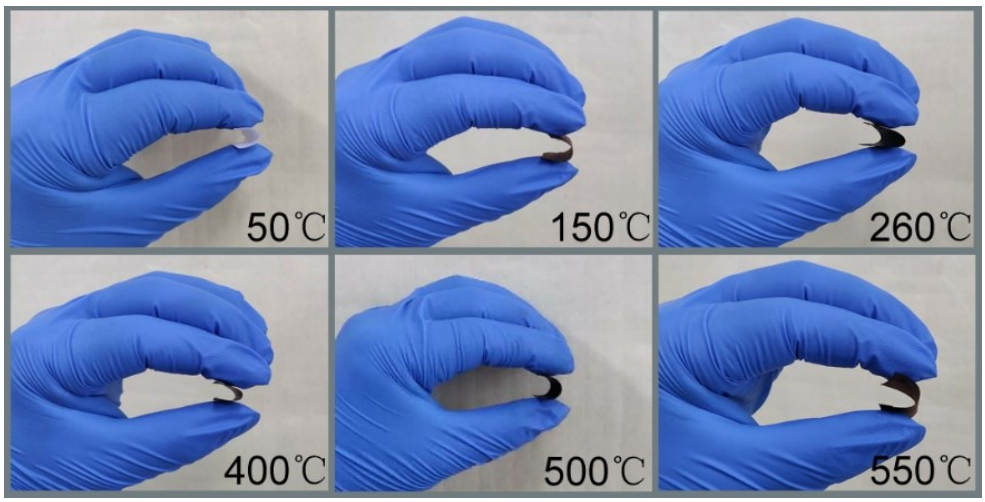

Fig. S2 Digital photos to show the bending of the fibrous membranes.

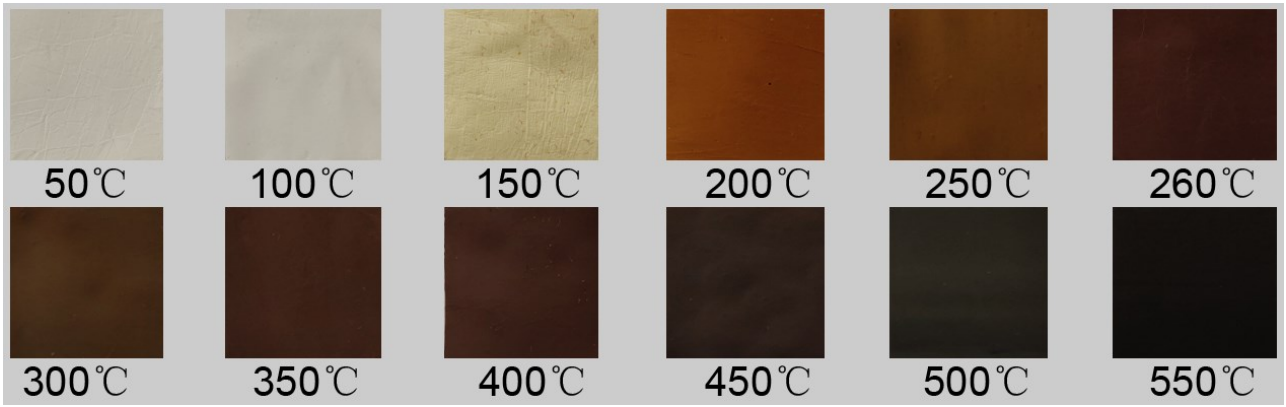

Fig. S3 Digital photos to show the appearance of the fibrous membrane after different treatment steps.

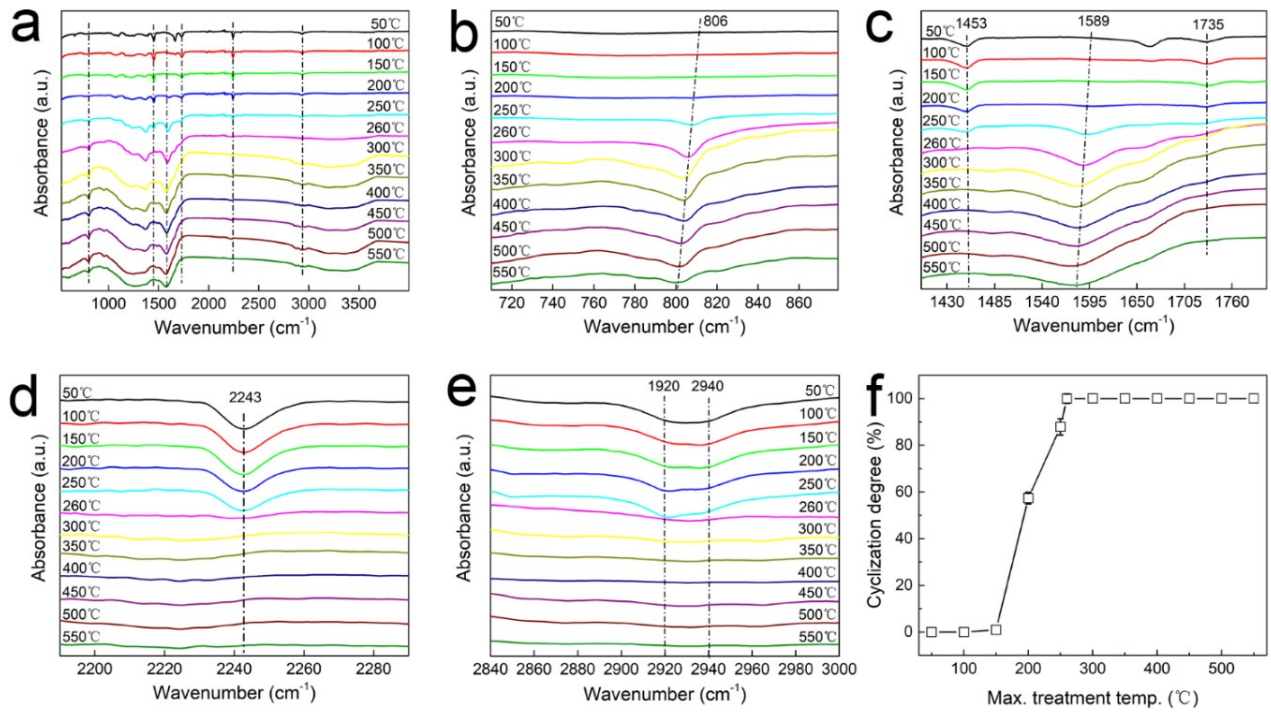

Fig. S4 (a-e) FTIR spectra of the PAN fibrous membranes treated by different temperatures; f) The degree of cyclization calculated from the integrated areas of the -C=N and -C≡N peaks.

Table S2, the assignment of the FTIR peaks

Peaks	Vibration groups
1453cm^{-1}, 2940cm^{-1}	-CH_2
1589 cm^{-1}	-C=N
1735cm^{-1}	-C=O
2243cm^{-1}	-C≡N
806 cm^{-1}	pyridine structure

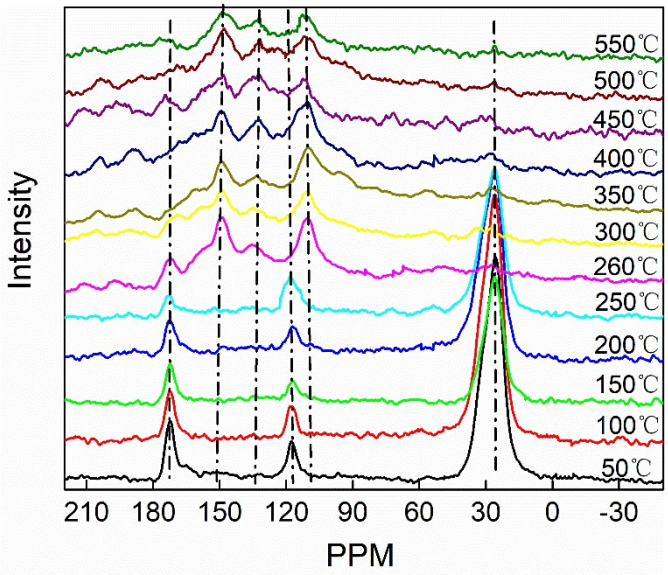

Fig. S5 Solid-state ^{13}C-NMR spectra of the PAN fibrous membranes treated at different temperatures.

The samples subjected to heat treatment above 260°C showed disappearance in -CN, -CH, and -CH_2 peaks, but the appearance of -C=N, -C=C, -C=CH. Thus, it indicates that PAN forms conjugated structures after heat treatment.

Table S3, assignment of the ^{13}C-NMR peaks

Peaks	Vibration groups
28 ppm	-CH, -CH_2
112 ppm	-C=C
119 ppm	-C≡N
133 ppm	-C=CH
150 ppm	-C=N
172 ppm	-C=O

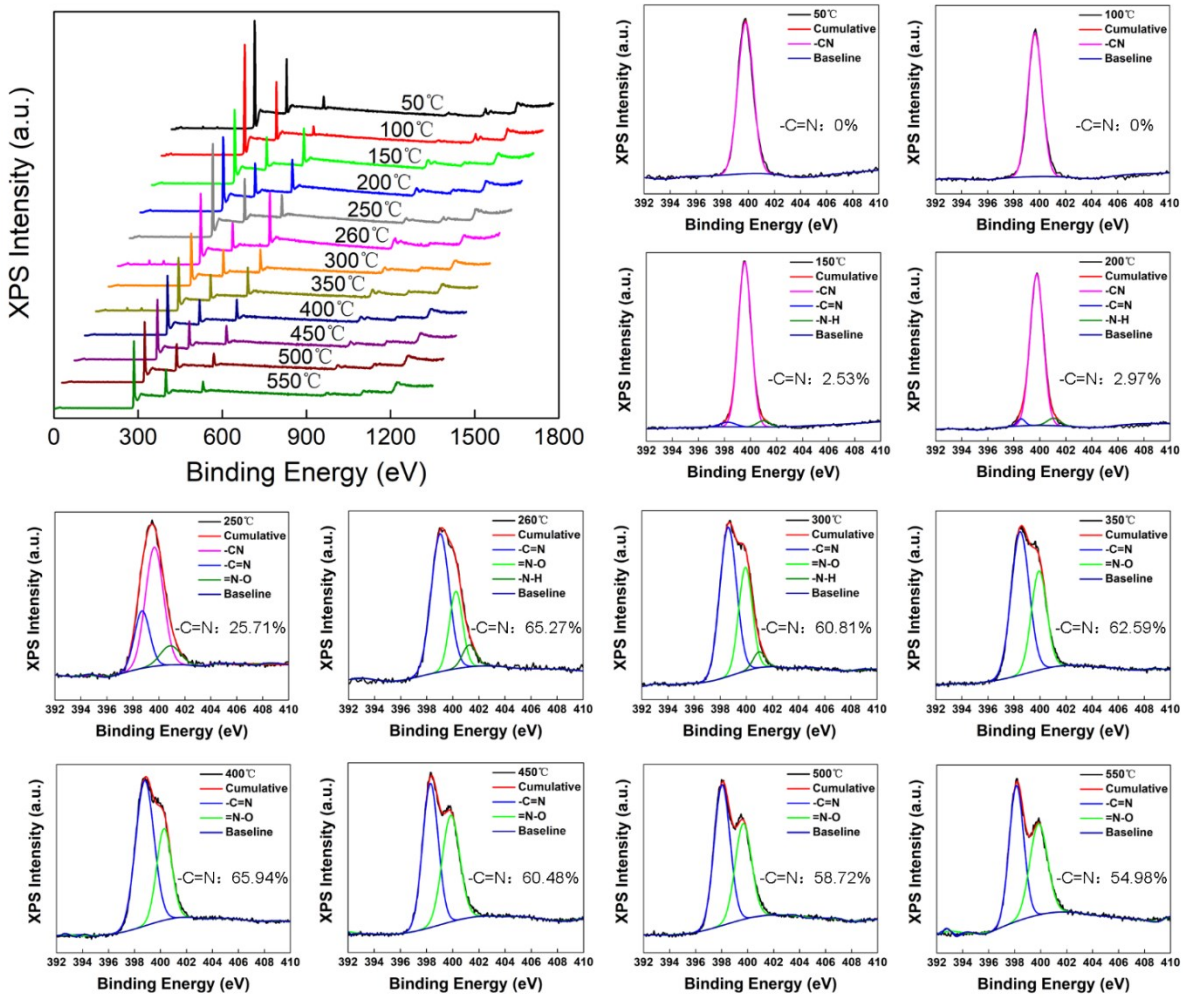

Fig. S6 XPS survey spectra and curve-fitted high-resolution N1s spectra of the PAN membranes.

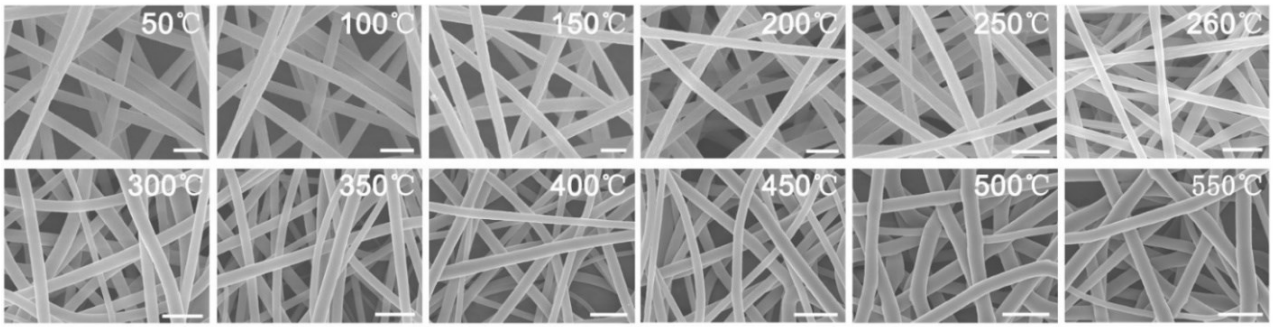

Fig. S7 SEM images of the PAN fibrous membranes at different treatment temperatures. (Solution concentration: 12%; Applied voltage: 23 kV; Spinning distance: 15 cm; flow rate of polymer solution: 0.5 ml/h; scale bar: 1 μm).

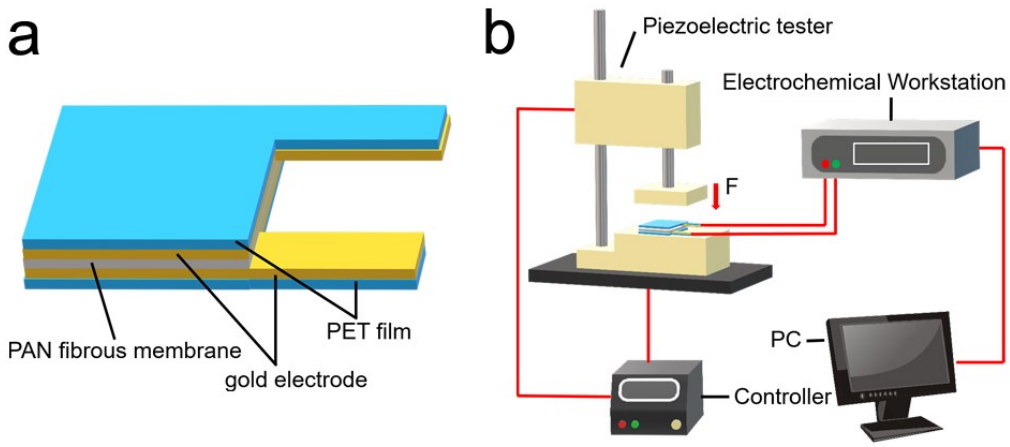

Fig. S8 Schematic diagrams of (a) piezoelectric device and (b) test system for measuring for electrical outputs at room temperature.

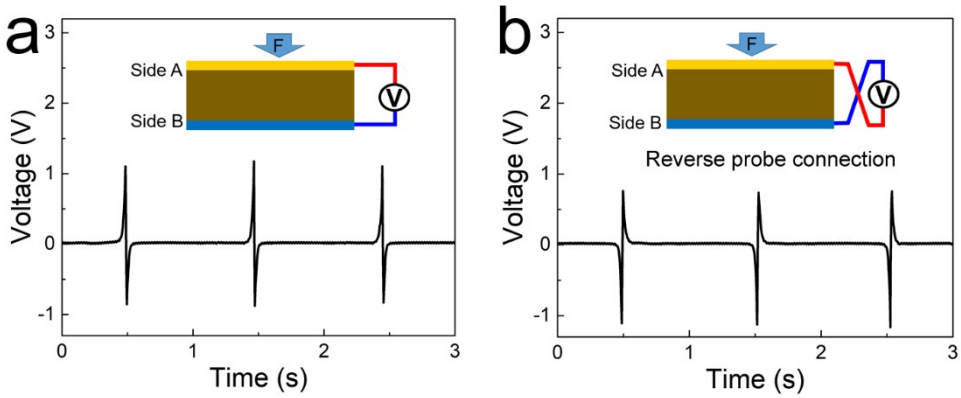

Fig. S9 Voltage outputs of a commercial PVDF piezoelectric film (manufactured by Measurement Specialties) in different electrode conditions.

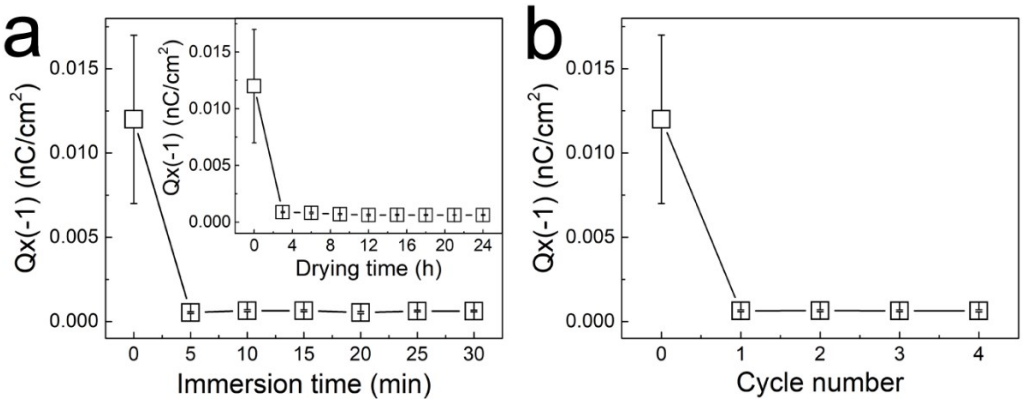

Fig. S10 (a) Effect of isopropanol immersion time on the electrostatic charge in the PAN membrane (inset, the effect of drying time on the residual charge, the membrane was immersed in isopropanol for 30 min before drying); (b) effect of the charge-removal treatment cycles on charges;

Fig. S10a shows the residual charges of the heat-treated PAN membrane (max heating temp 450 °C). After immersing in isopropanol for 30 minutes and drying at ambient conditions for 5 min, the charges on the nanofibers decreased significantly from 0.012 nC/cm^2 to 0.00062 nC/cm^2, reduced by over 90%. When the immersed sample was dried at ambient conditions for 24 hours, 97.5% of the charge was removed. Repeating the charge removal treatment (30 min immersion and 24-hour drying) showed a negligible reduction in the residual charge.

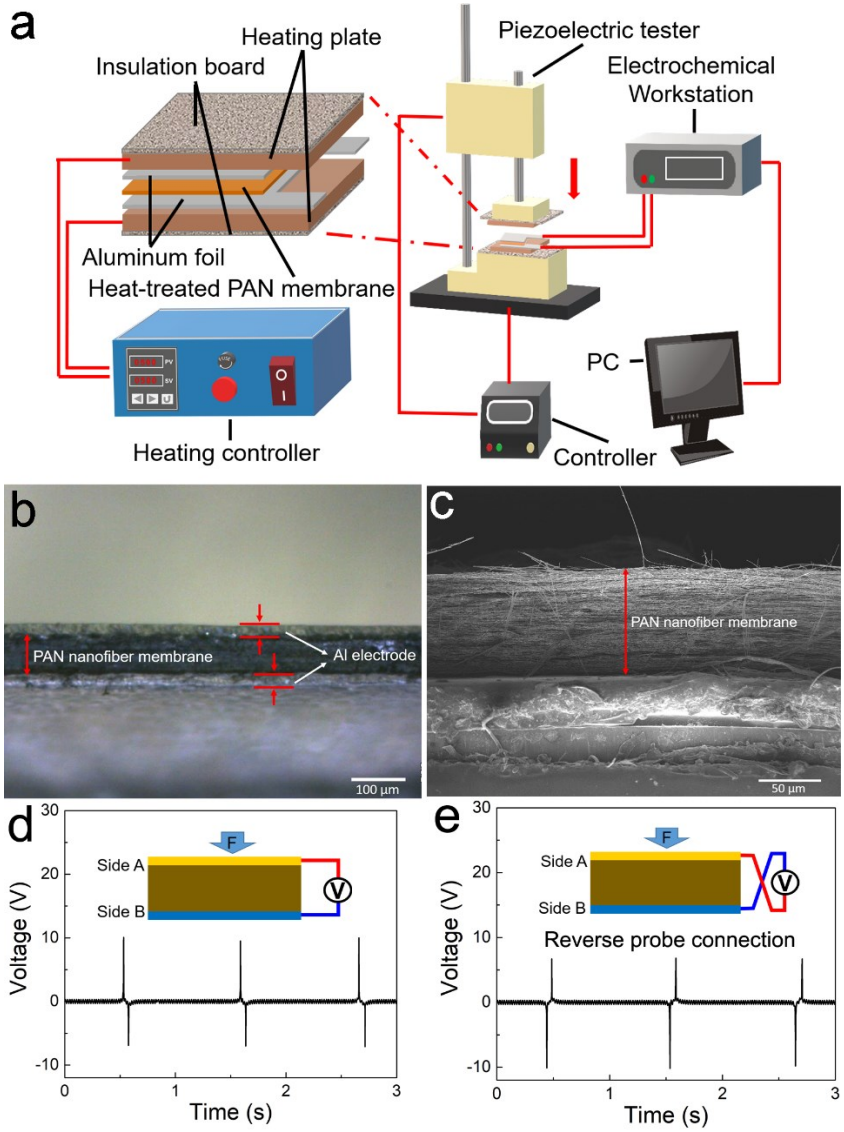

Fig. S11 (a) High-temperature piezoelectric testing system, (b) cross-sectional optical image of the piezoelectric device, (c) cross-sectional SEM image of the heat-treated PAN nanofiber membrane, (d) & (e) voltage outputs of the membrane device and effect of electrode connection on the output polarity (the test was at 450 °C).

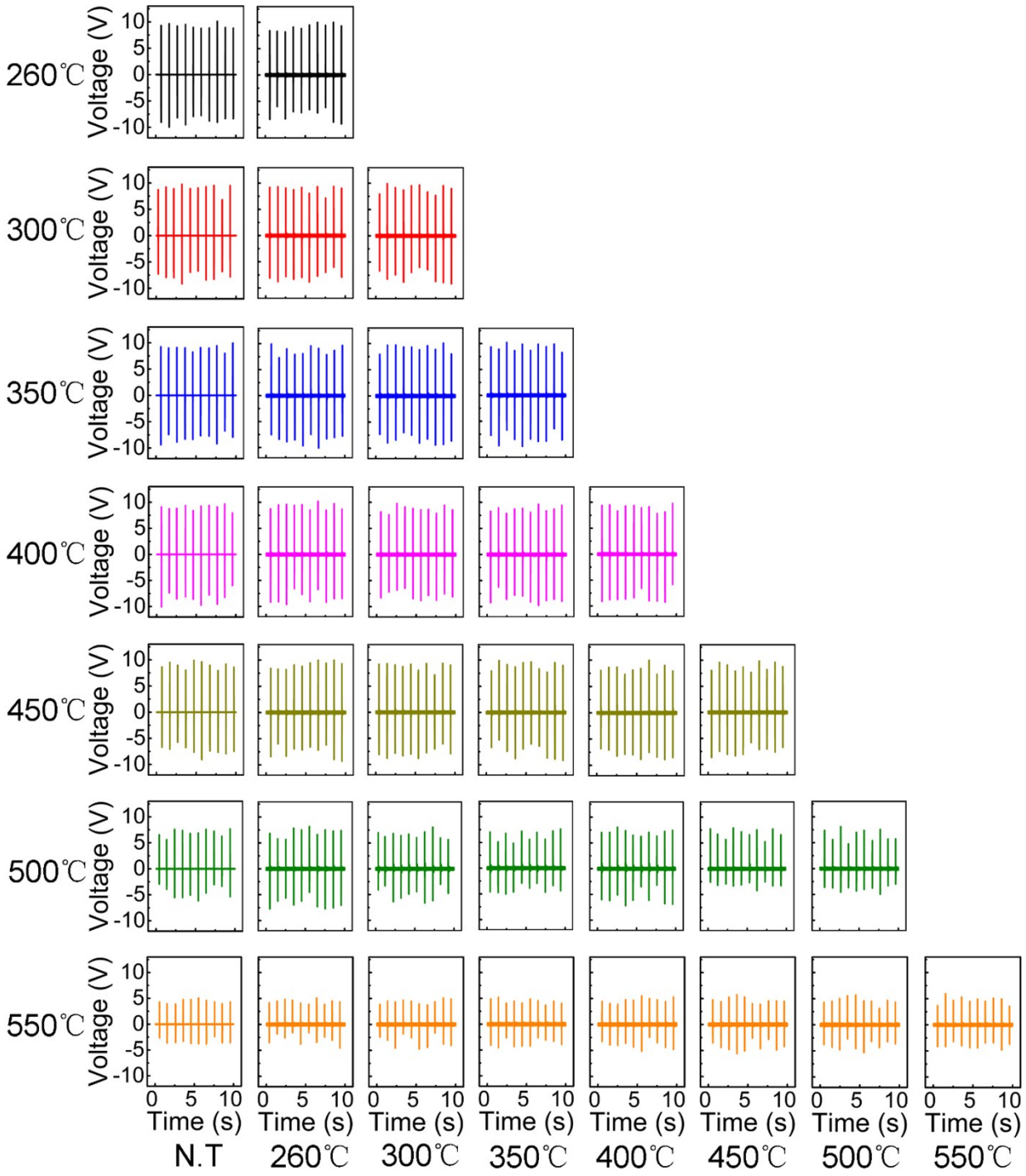

Fig. S12. The voltage output of the PAN fibrous membranes at a temperature below the highest processing temperature. All the tests were performed in an air atmosphere.

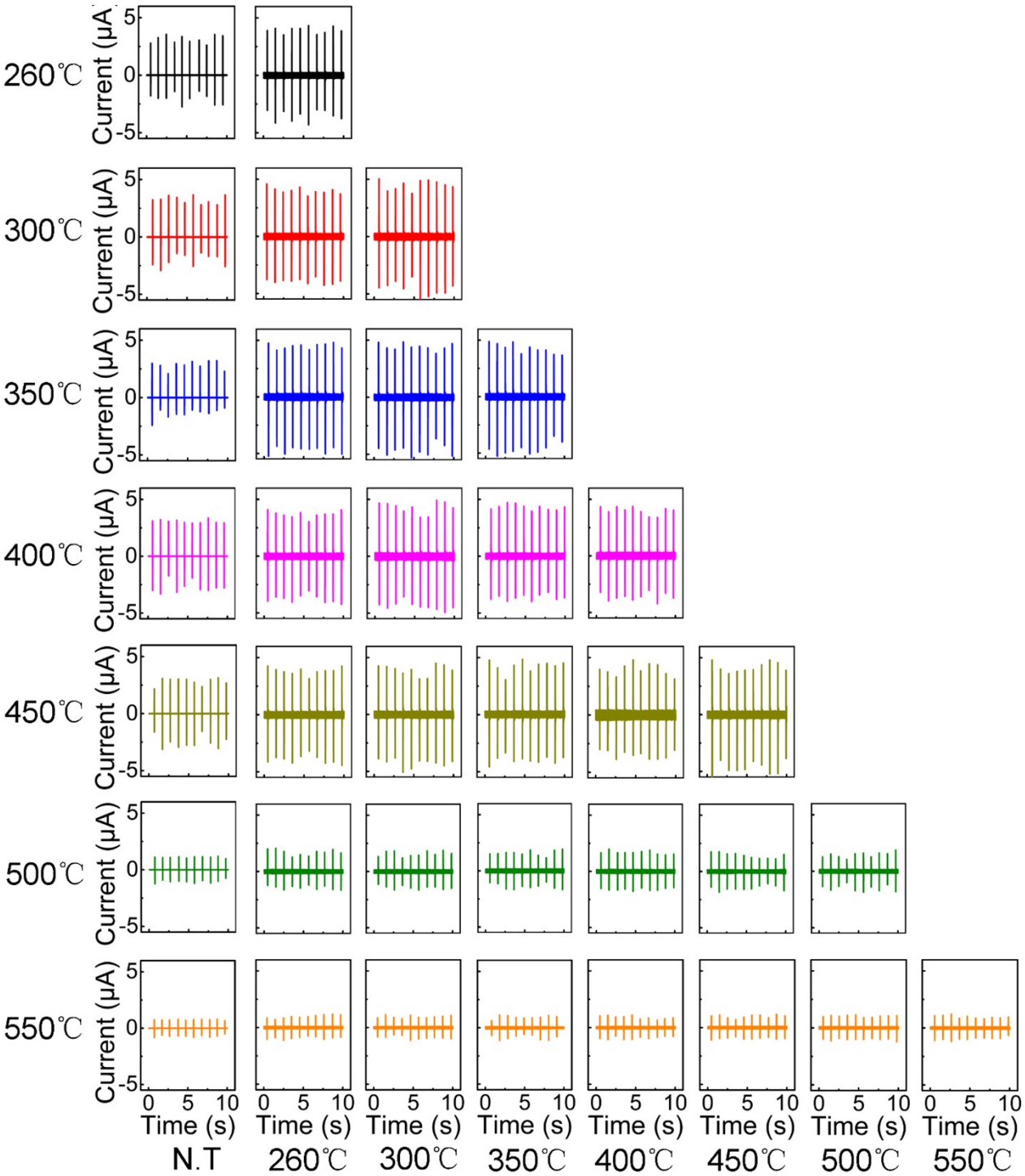

Fig. S13. The current output of the PAN fibrous membranes at a temperature below the highest processing temperature. All the tests were performed in an air atmosphere.

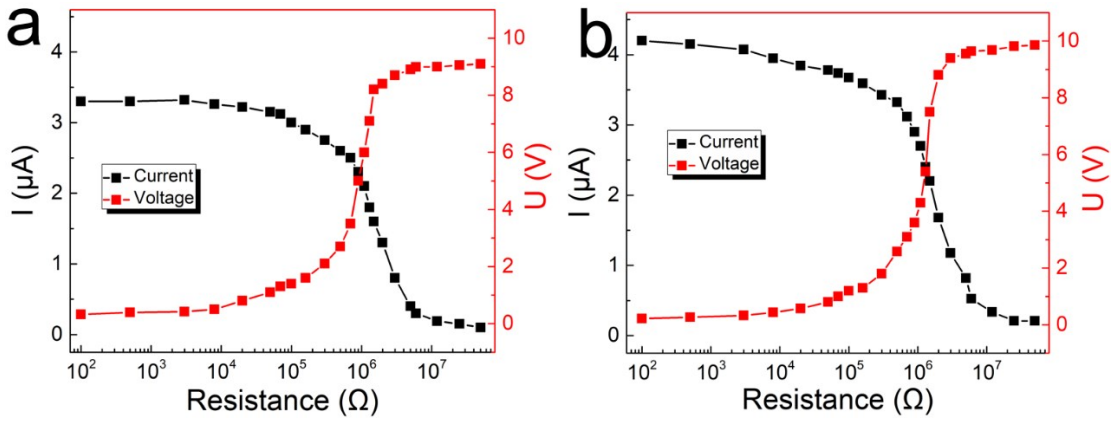

Fig. S14 Changing of PAN device current and voltage outputs with the external resistor loads. (a) The device working at (a) room temperature and (b) high-temperature (450 °C) conditions.

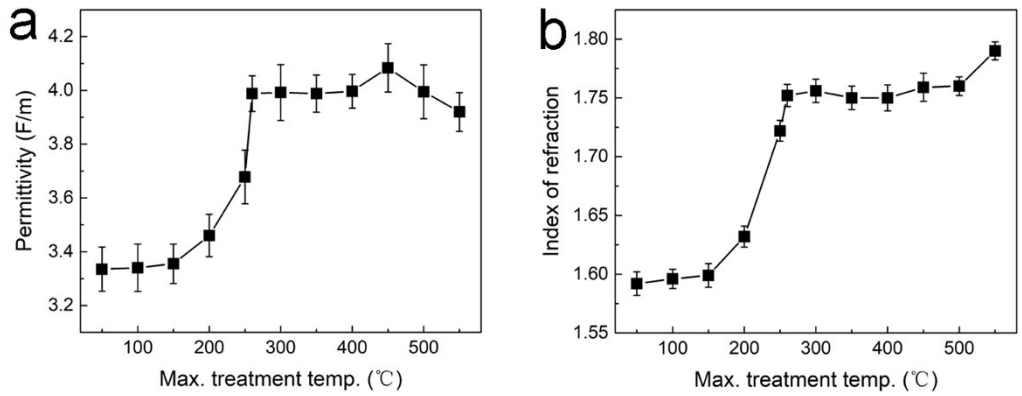

Fig. S15 the dielectric constant and refractive index for calculation of dipole moment of PAN films. The films were treated in the same process as the fibrous membranes, and the max temperature is the temperature the film experienced during the treatment process.

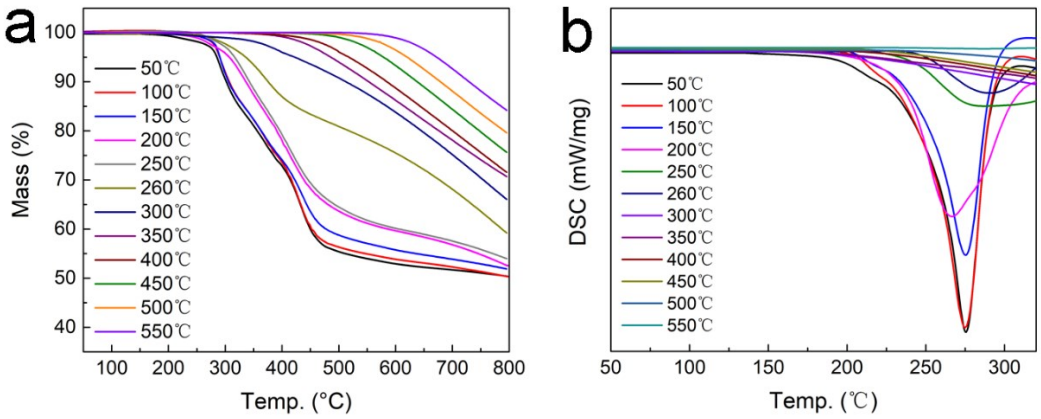

Fig. S16 TGA and DSC curves of the heat-treated PAN membranes.

References

S-1. L. Yang, Q. Zhao, Y. Hou, L. Hong, H. Ji, L. Xu, K. Zhu, M. Shen, H. Huang and H. He, *Composites Science and Technology*, 2019, **174**, 33-41.

S-2. Y. Sun, J. Chen, X. Li, Y. Lu, S. Zhang and Z. Cheng, *Nano Energy*, 2019, **61**, 337-345.

S-3. G. Jian, Y. Jiao, Q. Meng, Y. Guo, F. Wang, J. Zhang, C. Wang, K.-S. Moon and C.-P. Wong, *Nano Energy*, 2021, **82**, 105778.

S-4. C. Baur, Y. Zhou, J. Sipes, S. Priya and W. Voit, *Energy Harvesting and Systems*, 2014, **1**, 167-177.

S-5. M. Akiyama, Y. Morofuji, T. Kamohara, K. Nishikubo, Y. Ooishi, M. Tsubai, O. Fukuda and N. Ueno, *Advanced functional materials*, 2007, **17**, 458-462.

S-6. J. Gutiérrez, A. Lasheras, J. M. Barandiarán, J. L. Vilas, M. San Sebastián and L. M. León, *MRS Online Proceedings Library*, 2012, **1398**, 15-20.

S-7. X. Wen, Y. Su, Y. Yang, H. Zhang and Z. L. Wang, *Nano Energy*, 2014, **4**, 150-156.

S-8. A. Ahmed, M. F. El-Kady, I. Hassan, A. Negm, A. M. Pourrahimi, M. Muni, P. R. Selvaganapathy and R. B. Kaner, *Nano Energy*, 2019, **59**, 336-345.

S-9. Z. Qian, R. Li, J. Guo, Z. Wang, X. Li, C. Li, N. Zhao and J. Xu, *Nano Energy*, 2019, **64**, 103900.

S-10. D. P. Erhard, F. Richter, C. B. Bartz and H. W. Schmidt, *Macromolecular rapid communications*, 2015, **36**, 520-527.

S-11. X. Xi and D. Chung, *Carbon*, 2020, **160**, 361-389.

S-12. M. Sborikas, X. Qiu, W. Wirges, R. Gerhard, W. Jenninger and D. Lovera, *Applied Physics A*, 2014, **114**, 515-520.

S-13. E. Saarimaki, M. Paajanen, A. Savijarvi, H. Minkkinen, M. Wegener, O. Voronina, R. Schulze, W. Wirges and R. Gerhard-Multhaupt, *IEEE transactions on dielectrics and electrical insulation*, 2006, **13**, 963-972.